ISSN 0036-0244, Russian Journal of Physical Chemistry A, 2018, Vol. 92, No. 9, pp. 1762–1771. © Pleiades Publishing, Ltd., 2018.

PHYSICAL CHEMISTRY OF NANOCLUSTERS AND NANOMATERIALS

Optimizing Optical and Structural Properties of Nanocomposites by ZnO and BP-3[1]

M. Türemiş[a,*], İ. Ç. Keskin[b], M. İ. Katı[c], R. Kibar[b], K. Şirin[d], M. Çanlı[e], V. Çorumlu[f], and A. Çetin[b]

[a] *Department of Physics, Faculty of Engineering and Natural Sciences, Bursa Technical University, Bursa, Turkey*

[b] *Department of Physics, Faculty of Art and Science, Manisa Celal Bayar University, Manisa, Turkey*

[c] *Experimental Science Applications and Research Center (DEFAM)—Manisa Celal Bayar University, Manisa, Turkey*

[d] *Department of Chemistry, Faculty of Art and Science, Manisa Celal Bayar University, Manisa, Turkey*

[e] *Department of Chemistry and Chemical Processing Technologies, Mucur Vocational School, Ahi Evran University, Kırşehir, Turkey*

[f] *Department of Electric, Akhisar Vocational School, Manisa Celal Bayar University, Manisa, Turkey*

**e-mail: muratturemis@hotmail.com*

Received October 20, 2016; in final form, February 15, 2018

Abstract—This study aims to find out usage of zinc oxide (ZnO) and 2-hydroxy-4-methoxybenzophenone (BP-3) for getting better optical and structural properties of nanocomposites. Polymer nanocomposites were prepared by adding zinc oxide for minimizing UV rays effects of the sun with the particle size of nanometer in different ratios to a low density polyethylene (LDPE). The polymer mixtures were synthesized by mixing nanocomposite samples with BP-3 featuring UV stabilizer. Besides making tensile testing measurements, in order to find out the optical, structural, mechanical and thermal changes, the new polymer nanocomposites were characterized by XRD, TG-DTA spectra, and SEM images. The samples with zinc oxide which show luminescent properties were examined in terms of radioluminescence features. Radioluminescence spectrum showed characteristic peaks of zinc oxide dispersed nanocomposites prepared with LDPE. The intensity of the characteristic peaks at 530 and 390 nm (exciton) increased by increasing rates of nanopowder zinc oxide while adding BP-3 to the composites caused a decrease in intensity of radioluminescence.

Keywords: polymer nanocomposite, low density polyethylene, radioluminescence, optical absorption, structural characterization, mechanical properties, thermal analysis

DOI: 10.1134/S0036024418090315

INTRODUCTION

Polymers are the most promising alternative materials as compared to quite complex and expensive semiconductor of micro and nano electronics because of their availability and being low cost materials [1]. One of the most commonly used thermoplastics among polymers is polyethylene (PE) due to its toughness, near zero moisture absorption, perfect chemical inertness, low coefficient of friction, ease of processing and unusually electrical properties [2]. Generally, the most important polyethylene forms are low density polyethylene (LDPE), high density polyethylene (HDPE) and medium density polyethylene (MDPE). LDPE was chosen for this study because of its excellent flexibility and extensibility. Besides, it is widely used in food packaging materials and plastic film applications such as plastic bags and film wraps due to its excellent mechanical, chemical, processing and thermal properties [3–7].

Recent efforts about polymer studies show that it is popular to synthesize nanocomposites with the size of 1–100 nm [5–7]. Besides having reduced water and gas permeability, high thermal stability, flame resistance, recyclability, and ionic conductivity, electrical and mechanical properties of nanocomposites are also being improved. Polymer nanocomposites are synthesized with having higher performance by using nanometal and its oxide particles not only in the mechanical reinforcement, but also in optical, magnetic and electrical properties [8]. Nano-sized ZnO has a very broad range of applications from food packaging to the cosmetics industry [9, 10].

LDPE nanocomposite filled with ZnO nanoparticles lead to percolation at lower volume fraction, resulting in higher electrical conductivity [11–18]. Insulated nanoparticles raise the electrical conductivity of the nanocomposite with a better compactness by creating enhanced coupling among the nanoparticles through the grain boundaries [19]. Changing properties of polymers with ZnO cause modification of poly-

[1] The article is published in the original.

Table 1. Nomenclature, composition of nanocomposites (wt %)

Sample code	PE	ZnO	BP3
A1	100	—	—
A2	99	1	—
A3	97.5	2.5	—
A4	95	5	—
A5	90	10	—
A6	99.5	—	0.5
A7	98.5	—	1.5
A8	97.5	—	2.5
A9	94.5	5	0.5
A10	93.5	5	1.5
A11	92.5	5	2.5

mer by reduction in molecular weight [7]. Besides, UV radiation and ozone also cause serious degradation in the polymer materials. BP-3 (2-hydroxy-4-methoxybenzophenone to) is an effective UV stabilizer with high damping coefficient, and it can convert absorbed energy into heat without creating any chemical change [20]. Especially, using BP-3 is the reason for minimizing UV degradation in nanocomposites.

In this study, synthesis of ZnO–LDPE nanocomposites with modified by BP-3 was carried out. For this purpose, nanosized ZnO and BP-3 in different ratios were dispersed to LDPE. The synthesized nanocomposite samples were characterized by RL, optical absorption, XRD, mechanical testing (Elongation at Break, Tensile Strength at Yield, Tensile Strength at Break), thermal analysis (TG-DTA) measurements, and SEM images.

EXPERIMENTAL

Preparation of Nanocomposites

Low density polyethylene (I22-19T) was supplied as granular by Petkim Petrochemical Company (Aliaga, Izmir, Turkey). ZnO (<100 nm) and 2-hydroxy-4-methoxybenzophenone (BP-3) was purchased from Sigma Aldrich and Alfa Aeser, respectively. The nanocomposite samples were prepared from low density polyethylene (I22-19T) granules with different ratios of ZnO and BP-3 by using twin screw extruder (Collin ZK 25T). For each nanocomposite, components were well measured various ratios and thoroughly premixed in Table 1.

The nanocomposites were prepared by melting the mixed components in extruder which was set at; screw diameter: 25 mm; length to diameter ratio: 18 : 1; pressure: 8–10 bar; temperature scale for samples from filing part to head was 170–250°C and the screw operation speed was 30 rpm. Nanocomposites ratio and their codes are given in Table 1.

RESULT AND DISCUSION

Radioluminescence (RL)

The RL spectra were created in an X-ray unit with a Machlett OEG-50A tube running with a current of 15 mA and a voltage of 30 kV delivering a dose rate of 30 Gy min^{-1}. Luminescence detection system is conducted between 200 and 1200 nm with an integration time of 5 s with a Yobin Yvon spectrometer, coupled to a liquid nitrogen cooled CCD camera.

As shown in Fig. 1, the RL spectra at room temperature shows that luminescence spectrum for pure PE is not present (A1). However, when ZnO dispersed into PE with different percentage RL intensity has increased in proportion to the amount of ZnO (A2–A5). RL spectrum of ZnO was observed at approximately 530 nm to be similar to the bulk ZnO crystal form. This large peak with maximum point of ~530 nm shows that ZnO is a material having a crystalline blue-green light emission. Within ZnO between ~400 and 700 nm crystal there is a broad emission band observed because of the pollution created by V_O (oxygen vacancy), V_{Zn} (zinc vacancy), O_i (oxygen interstitial), Zn_i (zinc interstitial), and O_{Zn} (oxygen antisite) [12, 17]. Besides, at 390 nm there is a clear exciton peak for ZnO. With increasing amount of ZnO in PE, the intensity of exciton peak has gotten bigger. The peak shows a max at 1020 nm is the side peak caused by emission of the main peak.

Nanocomposite samples of A4 dispersed 5 wt % ZnO, UV stabilizer BP-3 was dispersed in the amount of 0.5 and 2.5 wt % (Fig. 2). While BP-3 amount increases the intensity of the RL peak belongs to ZnO decreases. It is believed that the X-ray exposured BP-3 led to the loss of energy by a non-radiative transition. Increase in the amount of BP-3 caused a decrease in the intensity of first and second peaks.

Optical Absorption

Optical absorption spectra of polymer matrix samples were recorded at room temperature in the wavelength region of 200–2000 nm using Perkin-Elmer Lambda 950 spectrophotometer.

The sharp edges of UV absorption spectra pointed out good crystallinity in the samples with ZnO powder [18]. According to Fig. 3, depending on the amount of ZnO in PE, the range and intensity of absorbed UV region sharply increased. In sample of A5, the absorption effect is being maximum between 340 and 400 nm.

The absorbed UV radiation energy by breaking most of the polymer bonds has caused free radical chain reactions which led to discoloration, embrittlement and ultimately degradation in polymer [20]. As shown in Fig. 4, in order to prevent degradation, the reaction of participating BP-3 UV stabilizer into the polymer seems to let the polymer absorb 320–400 nm

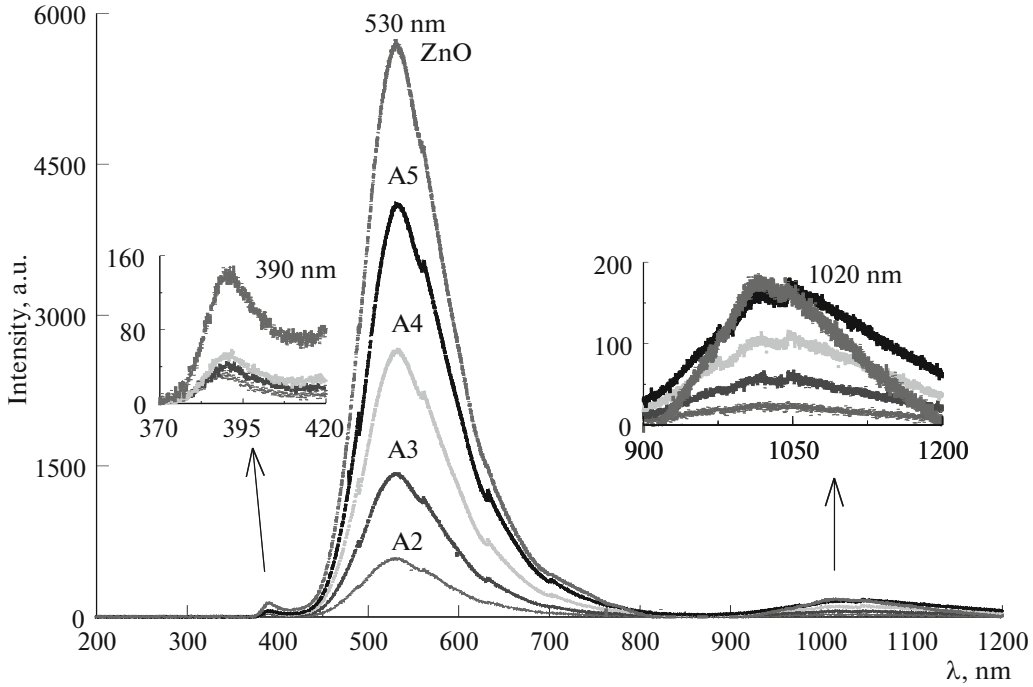

Fig. 1. RL spectra of ZnO and nanocomposites (A2–A5).

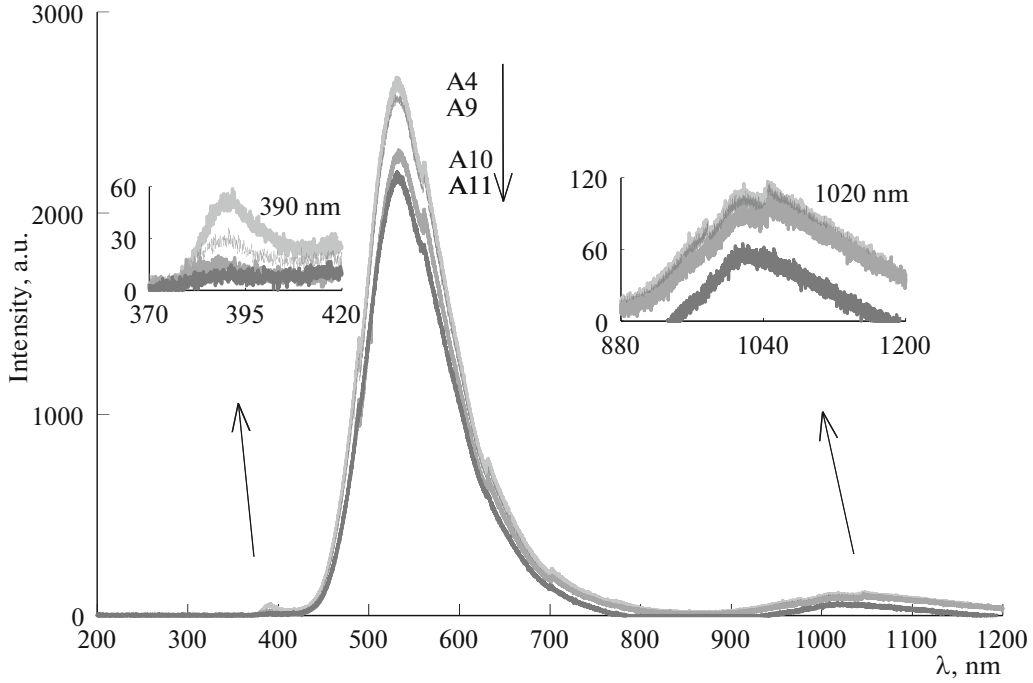

Fig. 2. RL spectra of nanocomposites (A4, A9, A10, A11).

range in the UV region in which pure polyethylene cannot prevent absorption.

Mechanical Testing Measurements

The tensile properties were examined using a Schimadzu tensile tester following the ASTM D-638 procedure and using type 4 test specimen dimensions. The crosshead speed was set at 50 mm min^{-1} and 5 samples were tested for each composition. Elongation at break of the samples was determined from the recorded stress versus strain curve. PE has been dispersed to improve the work ability and strength of

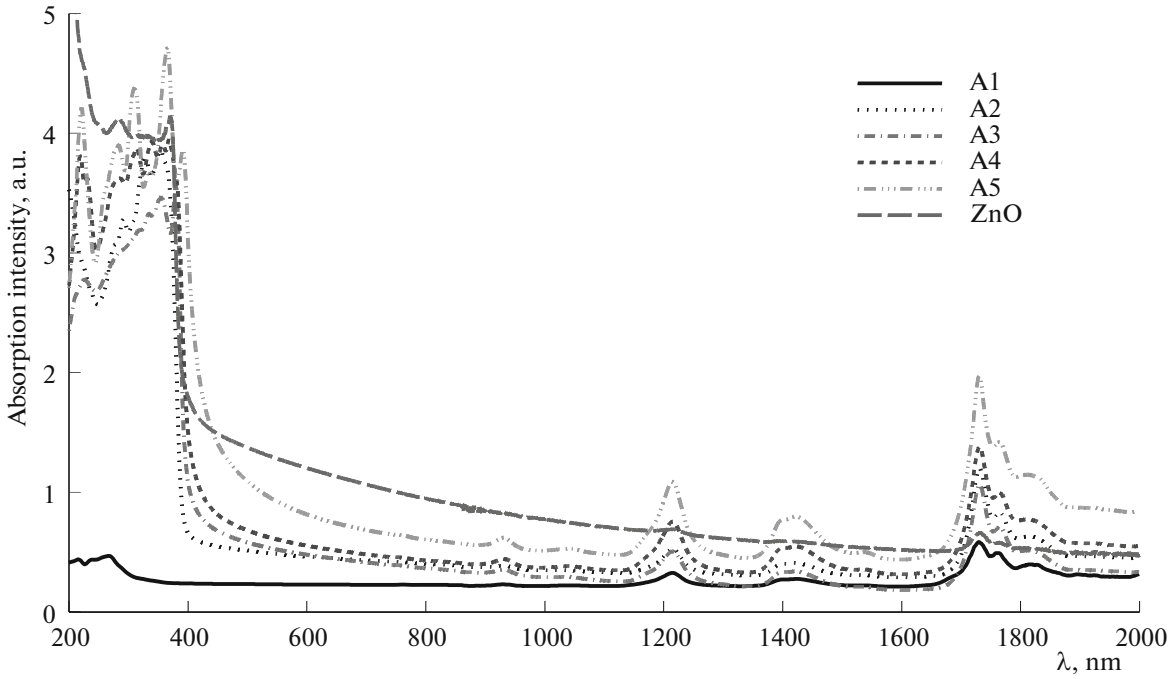

Fig. 3. Absorption peaks of ZnO and nanocomposites (A1–A5).

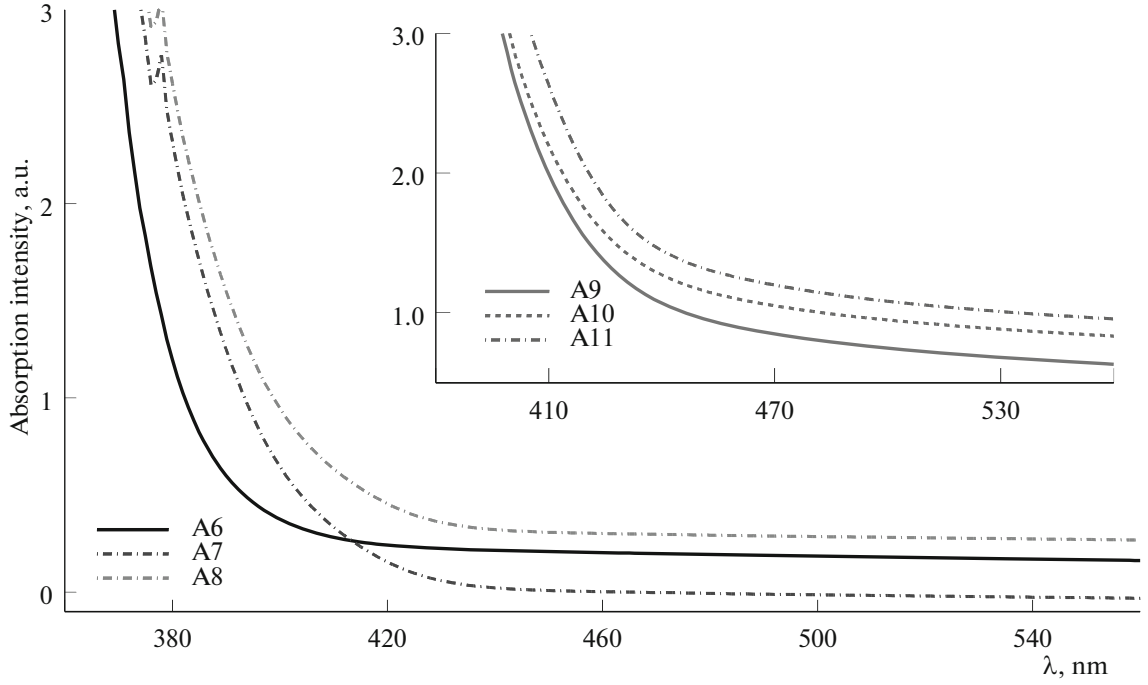

Fig. 4. Absorption peaks of nanocomposites (A6–A8) and (A9–A11).

thermoplastics [21, 22]. To reinforce polymers, nanoparticles are already being used in previous studies [23]. Mechanical and thermal properties of PE and PP are examined before and after they are mixed. The strength against breakage of PE was found higher than PP and PE mixture [24]. With increasing ratio of dispersed ZnO into PE, the amount of elongation at break is decreased (Table 2 and Fig. 5a).

A9–A10–A11 nanocomposites which are synthesized 5% ZnO dispersed nanocomposite A4 with BP-

Table 2. Mechanical properties of nanocomposites (C is elongation at break, F_1 and F_2 are tensile strength at yield and at break, respectively)

Sample code	A1	A2	A3	A4	A5	A6	A7	A8	A9	A10	A11
C, %	47.96	42.59	30.69	24.67	18.57	54.18	49.37	45.19	43.74	39.68	35.52
F_1, kg/cm^2	4.80	68.37	54.89	50.00	46.12	41.45	40.26	39.79	43.16	41.37	38.57
F_2, kg/cm^2	95.61	89.69	84.59	90.92	100.91	92.96	92.13	90.82	85.41	86.54	88.67

3 0.5, 1.5, and 2.5%, respectively, showed higher amount of % elongation than A4 sample obtained by only adding ZnO. As a matter of fact that increase in ZnO and BP-3% contribution rate caused reduction in elongation (Table 2 and Fig. 5b).

Figure 5a shows that elongation at break values of sample A6 and A7 is higher than sample A1 and A8 when BP-3 was dispersed in the amount of 0.5 and 1.5 wt %. Raising amounts of BP-3 in PE will cause a decrease in elongation at break values. In the same graph, the samples A9, A10, and A11 show higher values than A4 sample. In lights of elongation at break values, the influence of BP-3 has higher impact on PE than ZnO. The highest value for elongation at break was observed in the sample of A6 which has the lowest BP-3 ratio.

Tensile strength at yield is higher in nanocomposites with ZnO than the samples with BP-3 (Fig. 5b).

In Fig. 5c, tensile strength at break is getting lower in the sample of A2 and A3. The sample A4 and A5 show a sharp increase in tensile strength at break. While the samples of A6, A7, and A8 show a decrease, in the samples of A9, A10, and A11 there is an increase at the values of tensile strength at break. In other words, ZnO has positive impact on the values for tensile strength at break. BP-3 acts only placing with ZnO together in nanocomposites.

Thermal Analysis

Nanocomposite sample's differential thermal analysis (DTA) and thermo gravimetric (TG) were

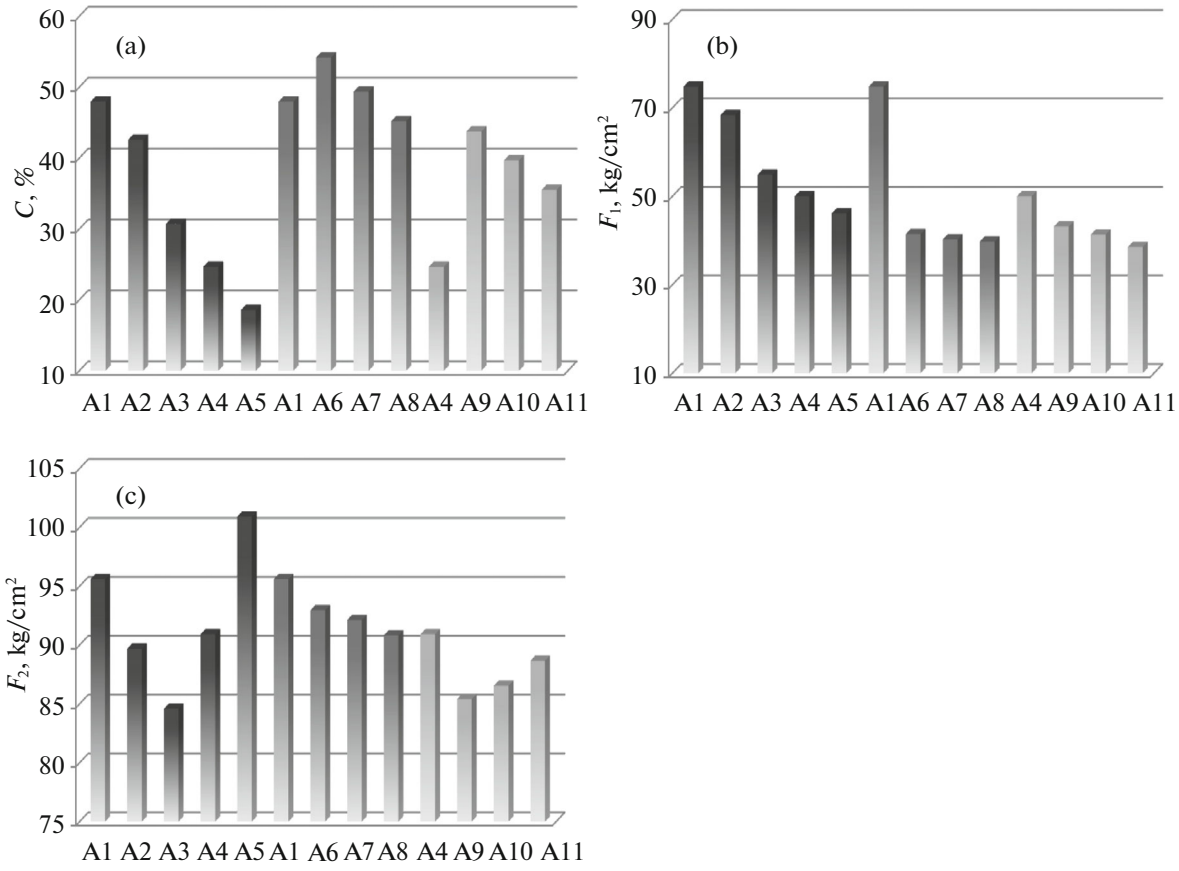

Fig. 5. Elongation at break graphs (a), tensile strength at yield graphs (b), and at break graphs (c) of nanocomposites.

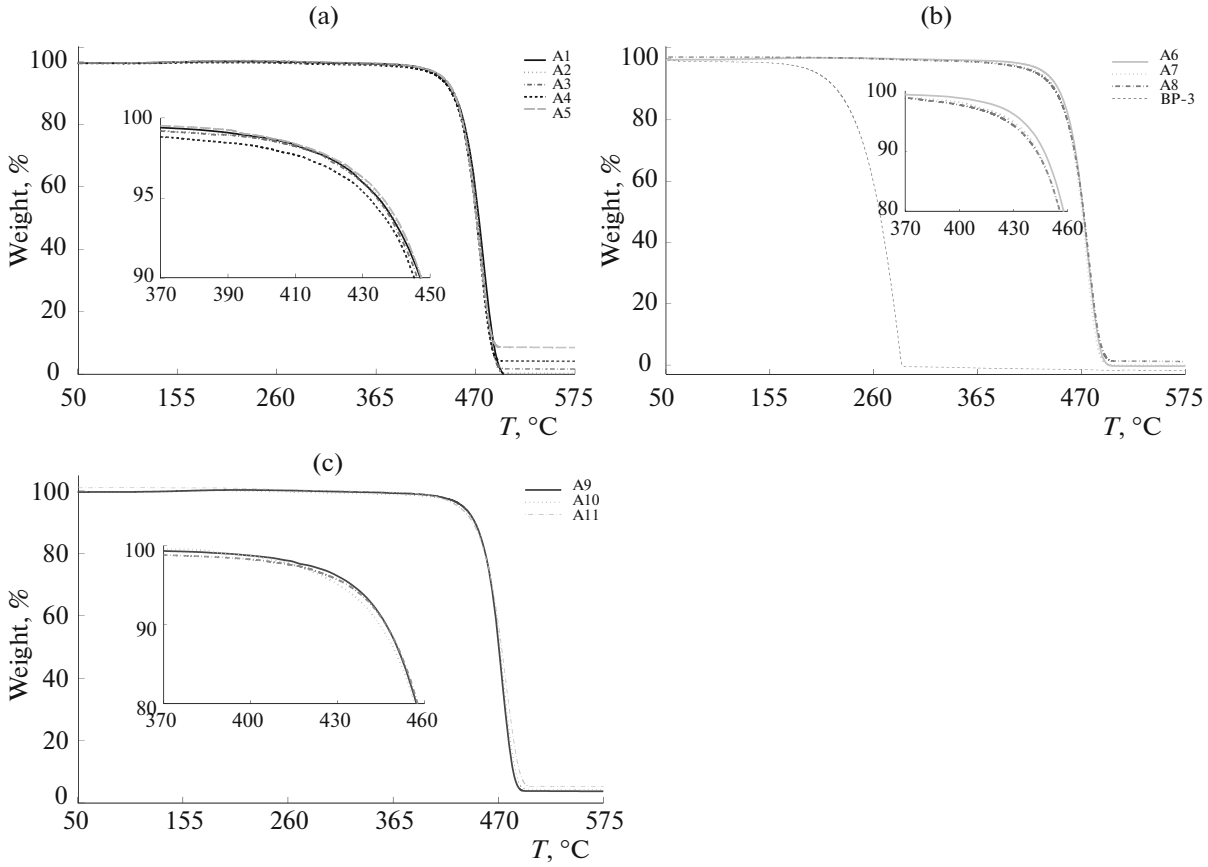

Fig. 6. TG Curves of nanocomposites A1–A5 (a), A6–A8 and BP-3 (b), A9–A11 (c).

carried out synchronously employing Hitachi SII Exstar 7300 thermal analyzer. The thermal behavior of nanocomposites was studied in the temperature range of 25–600°C at a heating rate of 10 K min^{-1} in air atmosphere. The results of TG and DTA thermal analysis are shown in Figs. 6 and 7. The TG analysis shows that nanocomposites exhibited sharp weight loss starting from 360–400°C and had no significant weight loss apart from the observed temperature. In DTA curves sharp exothermic peak observed at 110°C is assigned to the melting point of the nanocomposites. Another sharp exothermic peak observed at 478°C is assigned to decomposition, at this stage heavy weight loss in TG analysis has been noticed. Before melting there is no characteristic exothermic or endothermic peaks were observed. It is observed that there is no phase transition or decomposition up to the melting point. Sharpness of the exothermic peaks observed in DTA indicates good degree of crystallinity of the sample [25].

It is clearly seen in Fig. 6 that PE in nanocomposites was melted down and ZnO stayed solid because of having high melting point.

XRD (X-ray Diffraction)

X-ray diffraction of all materials was characterized by a Panalytical X-ray diffractometer with a CuK_α (λ = 1.541 Å) radiation source, equipped with a graphite monochromator. X-ray tube voltage and current were set at 45 kV and 40 mA, respectively. Fixed divergence slit size in X-ray generator is 0.4785°. All samples were positioned onto the sample loading plate located in the XRD chamber. Results of the patterns were obtained by step scanning from 20° to 80°. Patterns compared with the XRD card files of the Joint Committee on Powder Diffraction Standards (ref. code: 98-018-4793) [26]. The three most intensive peaks at 2θ = 31.7°, 34.4°, 36.2° were assigned to (100), (002), and (101) reflections of ZnO, indicating that samples were polycrystalline wurtzite structure [27].

In samples from A2 to A5, by increasing ZnO ratio in pure PE the characteristic peaks of ZnO have become more apparent (Fig. 8). Dispersed ZnO fills the gaps in the PE structure, and getting smaller *d*-spacing will decrease the intensity of peaks belonging PE. The peaks for BP-3 has not arisen through PE peaks because XRD peaks of PE overwhelmed BP-3.

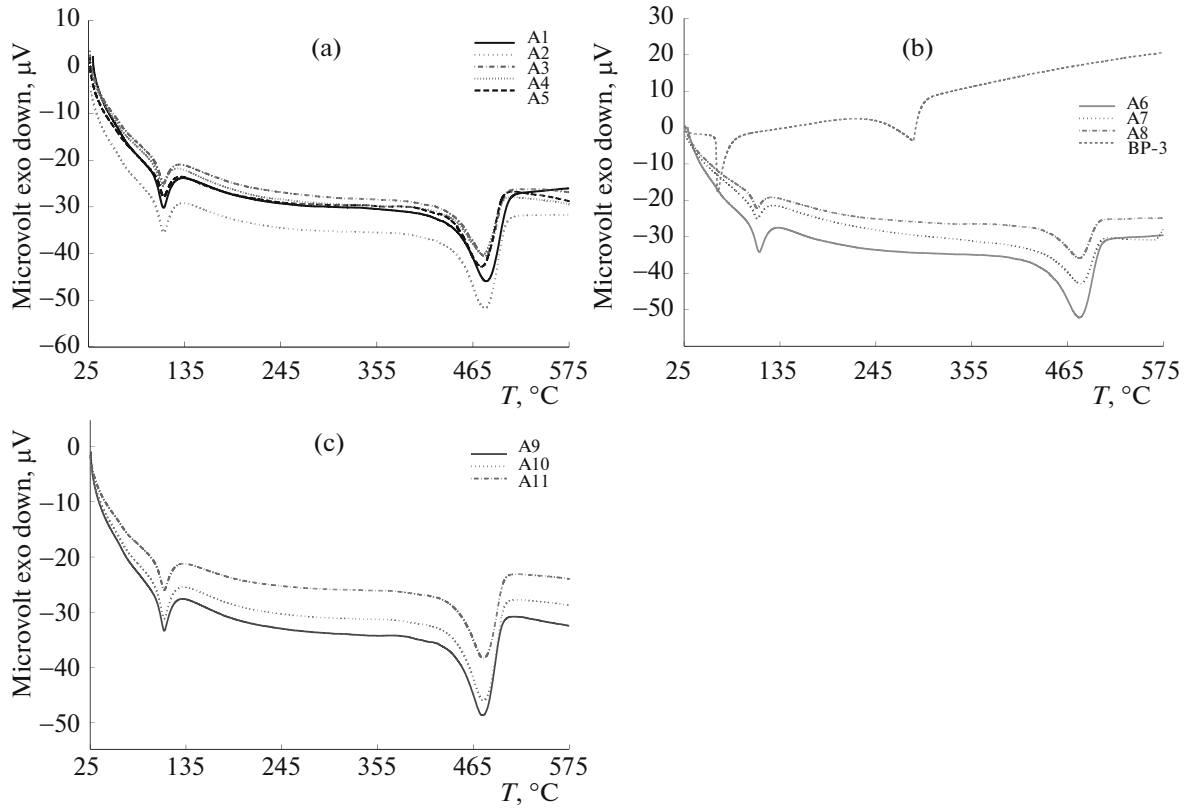

Fig. 7. DTA Curves of nanocomposites A1–A5 (a), A6–A8 (b), A9–A11 (c).

Scanning Electron Microscopy (SEM)

Scanning electron microscopy (SEM) was used to examine the morphology of nanocomposites by using a Philips XL-30S FEG e SEM. The SEM device was used in high vacuum mode with an acceleration voltage range of 2–5 kV, a resolution range of 3–100 μm and a magnification between ×1000–50000. Figure 9 shows the representative SEM micrographs taken for sample ZnO nanopowder, BP3 UV stabilizer and polymer nanocomposites (A3) and (A11).

Rod structures in ZnO are caused by morphological features of ZnO [27, 28]. This feature became more

Table 3. Thermal degradation values of polymer nanocomposites

Sample code	Degradation step, °C			Residue weight percentage		
	T_{start}	T_{max}	T_{end}	420°C	460°C	500°C
A1	399	473	497	2.32	21.93	99.79
A2	395	472	496	2.31	21.73	99.47
A3	396	471	575	2.43	24.18	98.04
A4	373	470	575	2.90	25.37	95.51
A5	400	470	575	2.24	24.60	91.19
A6	398	471	494	2.28	23.02	99.69
A7	387	472	493	3.16	25.77	99.61
A8	375	470	493	3.37	26.21	99.64
A9	396	470	575	2.39	24.10	95.97
A10	383	473	575	2.49	24.43	95.93
A11	360	471	575	2.78	23.14	95.37

T_{start} is started composition temperature based upon 1% weight loss, T_{max} is decomposition temperature based upon 50% weight loss, T_{end} is finished decomposition temperature based upon 99% weight loss.

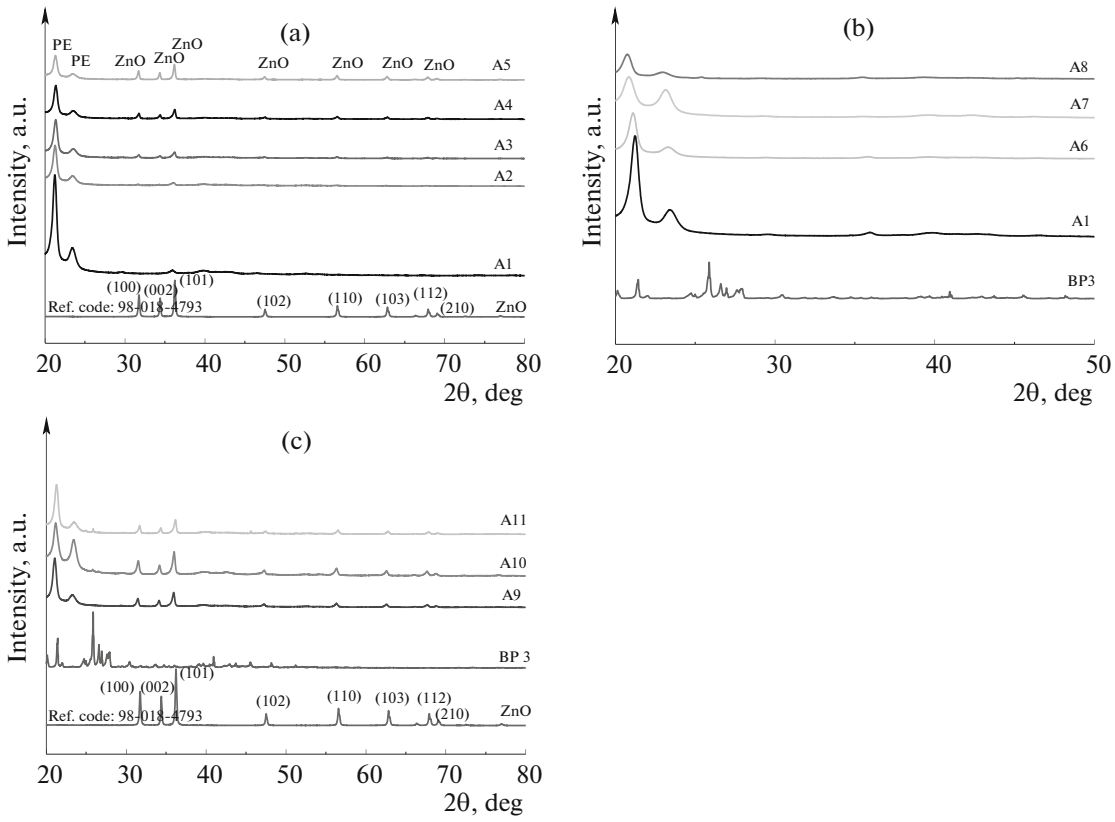

Fig. 8. XRD patterns of samples A1–A5 and ZnO (a), A1, A6 – A8, and BP3 (b), A9–A11, ZnO, and BP3 (c).

apparent as the contribution rate increased. The samples with BP-3 show increasing roughness and absorption. In A6, A7, and A8 samples which are only blended with BP-3 and PE, BP-3 appears not interacting with PE. However, for the sample A11 which has 5% ZnO and 2.5% BP-3 shows significant interface with ZnO. While some of the structures in BP-3 is broken, ZnO is taken their places. The new structured samples showed too much roughness in SEM, and their SEM images have taken the shape of a storm. The absorption rate in the samples showed a maximum in the absorption curves.

CONCLUSION

RL spectra of nanopowder ZnO and nanocomposites showed characteristic peaks of ZnO at 390, 530, and 1020 nm. At 390 nm a luminescence exciton peak is observed, at 530 nm it is the main peak on that ZnO and nanocomposites scatter blue-green light and at 1020 nm there is a secondary peak occurred by the main peak.

The RL intensity of the nanocomposites is increased by cumulative amount of ZnO in PE. On the other hand, the intensity of RL declines with increasing ratio of BP-3 in nanocomposites. The reason for this drop was that X-ray exposed BP-3 showed a non-radiative transition. Even though BP-3 is not a luminescent material, it is an agent showing good absorption in UV region. With smaller amount of ZnO and BP-3, undesirable UV beams do not pass through the nanocomposites. It is clearly seen that raising ratio of ZnO and BP-3 causes greater UV absorption field.

In mechanical test, for elongation at break, the nanocomposites with BP-3 has better treatment over the nanocomposites with ZnO. The values of tensile strength at yield are higher in the nanocomposites with ZnO than the ones with BP-3. According to the tensile strength at break graph, BP-3 only impacts positively when it is used with ZnO in PE.

In thermal analysis of the nanocomposites, PE is dominant over BP-3 and ZnO. It is clearly stated that characteristic peaks for BP-3 and ZnO in the nanocomposites were not observed. However, because of its high melting point, ZnO has still stayed in the nanocomposites without any degradation.

The characteristic peaks for ZnO has been more apparent with the raising ratio of ZnO in the nanocomposites in XRD graphs. The lower intensity of PE peaks in the nanocomposites is caused by ZnO filling the gaps in the structure of PE.

SEM images pointed out that nanopowder ZnO is in the form of rod structure occurred in the nanocomposites. With the raising amount of ZnO and BP-3 in

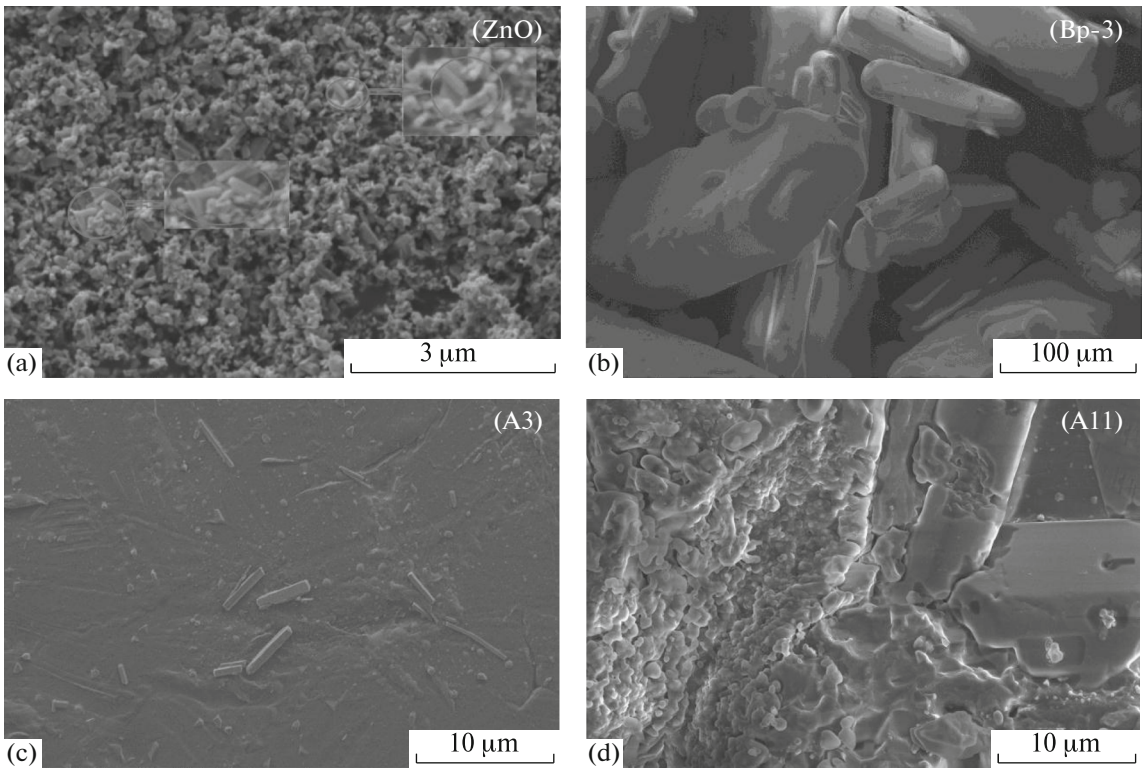

Fig. 9. SEM images of ZnO, BP-3, and nanocomposites (A3, A11).

the nanocomposites, the roughness is increased which points out the greater absorption rate. The best yield ratio in the nanocomposite is obtained in the state of maximum rate of ZnO and BP-3 in the nanocomposite.

As a conclusion, ZnO and BP-3 has increased the properties of nanocomposites and the nanocomposites with ZnO has generally higher values on optical and structural properties than the nanocomposites BP-3.

REFERENCES

1. M. Niklaus, PhD Thesis No. 4798 (2010)
2. P. N. Khanam and M. A. AlMaadeed, Adv. Manufact.: Polym. Comp. Sci. **1**, 63 (2015).
3. M. A. AlMaadeed, M. Ouederni, and P. N. Khanam, Mater. Des. **47**, 725 (2013).
4. E. E. M. Ahmad and A. S. Luyt, Compos., Part A **43**, 703 (2012).
5. J. Z. Liang, R. K. Y. Li, and S. C. Tjong, Polym. Test. **16**, 529 (1998).
6. K. Sirin, PhD Thesis (Ege Univ. Graduate School Nat. Appl. Sci., Izmir, Turkey, 2008).
7. J. D. Badia, E. Strömberg, S. Karlsson, and A. R. Greus, Polym. Degrad. Stab. **97**, 98 (2012).
8. S. Li, M. M. Lin, M. S. Toprak, D. K. Kim, and M. Muhammed, Nano Rev. **1**, 5214 (2010).
9. H. M. C. de Azeredo, Trends Food Sci. Tech. **30**, 56 (2013).
10. F. Beigmohammadi, S. H. Peighambardoust, J. Hesari, S. A. Damirchi, S. J. Peighambardoust, and N. K. Khosrowshahi, LWT - Food Sci. Tech. **65**, 106 (2016).
11. G. N. Panin, A. N. Baranov, and T. W. Kang, in *Proceedings of the 2nd International Conference on Advanced Optoelectronics and Lasers, 2008,* p. 700915
12. A. Cetin, R. Kibar, M. Ayvacıklı, N. Can, Ch. Buchal, P. D. Townsend, A. L. Stepanov, T. Karali, and S. Selvi, Nucl. Instrum. Methods Phys. Res., Sect. B **249**, 474 (2006).
13. J. Qu, Y. Zhu, Z. Chen, N. Yuan, and J. Ding, Russ. J. Phys. Chem. A **90**, 1621 (2016).
14. S. Klubnuan, S. Suwanboon, and P. Amornpitoksuk, Opt. Mater. **53**, 134 (2016).
15. H. S. Bhatti, K. Singh, Kavita, S. Kumar, and R. K. Choubey, Russ. J. Phys. Chem. A **88**, 1166 (2014).
16. Z. J. Mo, Z. H. Hao, H. Z. Wu, Q. Yang, P. Zhuo, H. Yang, J. P. Xu, X. S. Zhang, and L. Li, J. Lumin. **175**, 232 (2016).
17. N. Tu, K. T. Nguyen, D. Q. Trung, N. T. Tuan, V. N. Do, and P. T. Huy, J. Lumin. **174**, 6 (2016).

18. L. C. Ann, S. Mahmud, A. Seeni, S. K. M. Bakhori, A. Sirelkhatim, D. Mohamad, and H. Hasan, J. Environ. Chem. Eng. **3**, 436 (2015).

19. M. Ashby, P. Ferreira, and D. Schodek, *Nanomaterials, Nanotechnologies, and Design* (Elsevier, Amsterdam, 2009), p. 241.

20. J. R. Fried, *Polymer Science and Technology,* 2nd ed. (Nick Radhuber Pearson Education, MA, 2008), p. 263.

21. R. D. Deanin, M. A. Manio, C. H. Chuang, and K. N. Tejeswi, *Polyolefin Polyblends* (Marcel Dekker, Univ. Massachusetts, Lowell, MA, 2000), 613.

22. K. Sirin and M. Balcan, Polym. Adv. Technol. **21**, 250 (2010).

23. P. Hine, V. Broome, and I. Ward, Polymer **46**, 10936 (2005).

24. A. H. I. Mourad, Mater. Des. **31**, 918 (2010).

25. T. Suthan, N. P. Rajesh, C. K. Mahadevan, and G. Bhagavannarayana, Spectrochim. Acta, Part A **78**, 771 (2011).

26. R. P. S. Chakradhar, B. M. Nagabhushana, C. Shivakumara, J. L. Rao, S. C. Sharma, H. Nagabhushana, M. K. Kokila, and A. J. Reddy, Mater. Chem. Phys. **133**, 876 (2012).

27. M. Kahouli, A. Barhoumi, A. Bouzid, A. Al-Hajry, and S. Guermazi, Superlatt. Microstruct. **85**, 7 (2015).

28. A. Peles, V. P. Pavlovic, S. Filipovic, N. Obradovic, L. Mancic, J. Krstic, M. Mitric, B. Vlahovic, G. Rasic, D. Kosanovic, and V. B. Pavlovic, J. Alloys Compd. **648**, 971 (2015).